

## 2.1. Experiment

This chapter describes the experimental methodology utilized to synthesize the materials and provides specifics regarding the tools and techniques employed in the current work to investigate several properties, including structural, dielectric, electric, and impedance behaviour. In the field of electronic ceramics, materials research includes the following steps: Synthesis of different compositions in the system of interest; (ii) Crystal phase analysis; (iii) Heat treatment at high temperature; and (iv) Microstructural and dielectric behavior of the obtained samples. In the present investigation, various samples in diverse systems are synthesized through semi wet route,

- (a)  $\text{Bi}_{(2/3-x)}\text{Nd}_x\text{Cu}_3\text{Ti}_4\text{O}_{12}$  (BNCTO) with ( $x = 0.05, 0.10$  and  $0.20$ )
- (b)  $\text{Bi}_{(2/3-x)}\text{Sm}_x\text{Cu}_3\text{Ti}_4\text{O}_{12}$  (BSCTO) with ( $x = 0.05, 0.10$  and  $0.20$ )
- (c)  $\text{Bi}_{(2/3-x)}\text{Gd}_x\text{Cu}_3\text{Ti}_4\text{O}_{12}$  (BGCTO) with ( $x = 0.05, 0.10$  and  $0.20$ )
- (d)  $\text{Bi}_{(2/3-x)}\text{Dy}_x\text{Cu}_3\text{Ti}_4\text{O}_{12}$ (BDCTO) with ( $x = 0.05, 0.10$  and,  $0.20$ )

All the above-produced materials were characterized using several techniques, including powder X-ray diffraction, scanning electron microscopy (SEM), energy dispersive X-ray spectroscopy (EDX), and atomic force microscopy (AFM). The dielectric, electric, and impedance properties of several materials were tested using an LCR meter at certain frequencies and temperatures ranging from 300 to 500 K.

To synthesize the various compositions in the stated above system, we employed high purity raw materials such as bismuth nitrate, neodymium oxide, samarium oxide, gadolinium oxide, copper acetate, titanium dioxide, and citric acid, as specified in Table 2.1.

**Table 2.1** Specification of the chemicals used.

Raw Materials	Minimum Assay	Manufacturer
Bismuth nitrate, $\text{Bi}(\text{NO}_3)_3 \cdot 5\text{H}_2\text{O}$	99%	Merck, India
Copper acetate, $\text{Cu}(\text{CH}_3\text{COO})_2 \cdot \text{H}_2\text{O}$	99%	Merck, India
Samarium oxide, $\text{Sm}_2\text{O}_3$	99.99%	Merck, India
Gadolinium oxide, $\text{Gd}_2\text{O}_3$	99.99%	Aldrich, India
Neodymium oxide, $\text{Nd}_2\text{O}_3$	99.99%	Aldrich, India
Titanium oxide, $\text{TiO}_2$	98.5%	Merck, India
Citric acid, $\text{C}_6\text{H}_8\text{O}_7 \cdot \text{H}_2\text{O}$	99.5%	Merck, India

## 2.2. Material Synthesis

Doped BCTO was produced utilizing the semi-wet route approach. Materials have been turned into pellets to evaluate their bulk characteristics.

### 2.2.1. Semi Wet Route

The semi-wet approach, which is a modification of the sol-gel method, falls within the category of combustion synthesis techniques. Combustion synthesis is used to create multi-component, single-phase materials. This procedure is based on a redox reaction aided by an oxidant found in the precursor solution. In this procedure, all metal nitrate and acetate were taken in a stoichiometric molar ratio, and the solution was made using double distilled water, which also contained solid  $\text{TiO}_2$  powder. An accurately measured quantity of citric acid solution, equivalent to the metal ion present, was introduced into the above mentioned solution comprising nitrate and acetate. Citric acid, glycine, urea, ethylene glycol, and other metal nitrates are commonly employed as fuels and oxidants. Chelating chemicals, such as glycine,

oxalic acid, and others, can form complexes with metal ions in the precursor solution and act as fuel. Using a hot plate magnetic stirrer, the solution was heated at 70-80 °C to evaporate the water. This produced a viscous gel that, when heated further, self-ignites and releases a large volume of gasses. The dry powder that is obtained as the precursor is calcined at 800 °C for 6 h in a muffle furnace. After that, a mortar and pestle are used to reground the calcined powder until a fine powder is achieved. The obtained powder is uniformly mixed with a 2% polyvinyl alcohol (PVA) solution, which acts as a suitable binder. Then, it is pressed into cylindrical pellets using a hydraulic press, applying a pressure of 4-5 tons for 1 minute. The resulting pellets are gradually heated at 773 K to eliminate the PVA and then sintered at 1173 K for 8 hours. The flow chart presented in Figure 2.1 illustrates the sequential steps involved in preparing these materials using the specified preparation method [1].

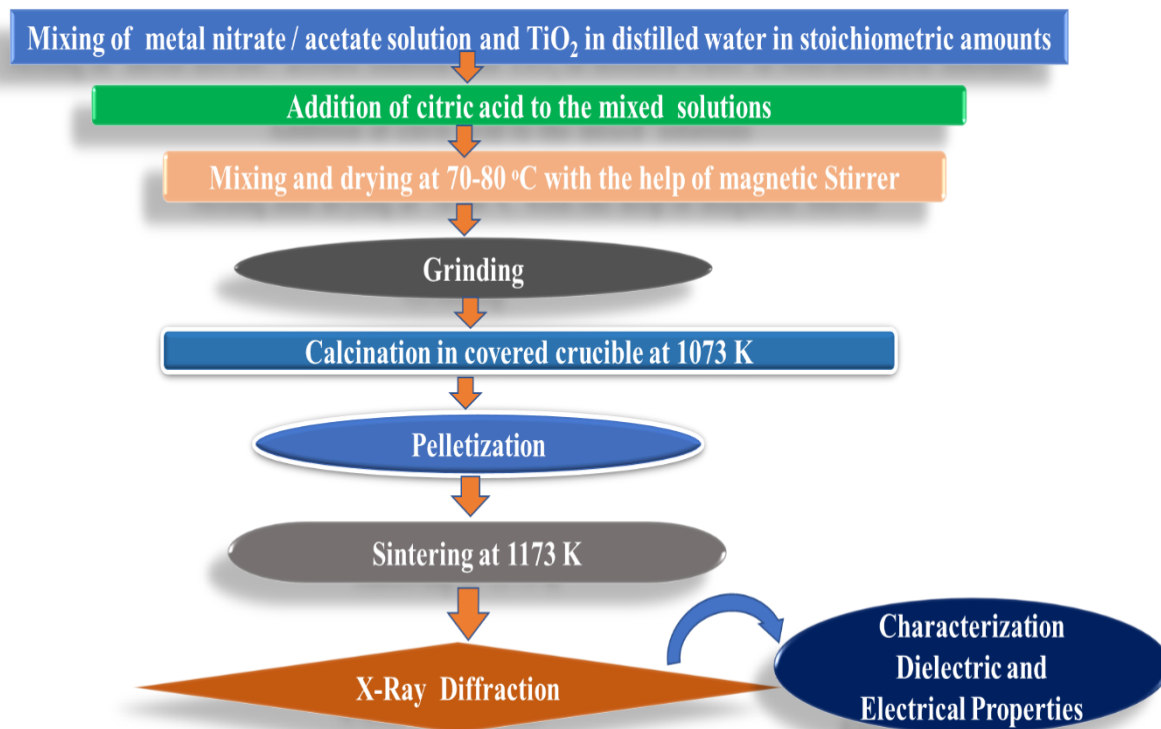


**Fig. 2.1.** Flow chart for the synthesis of complex perovskite by the semi-wet route.

### **2.2.2. Calcination Process**

Calcination is the process that heats starting materials to promote chemical reactions between constituent particles, leading to the creation of partial or full compounds through diffusion. Oxide materials are often calcined at temperatures over 500°C. Optimizing the calcination temperature for optimal characteristics is crucial for many materials. Calcination produces desirable single-phase material while removing moisture and other organic components. In the current work, the synthesized materials were calcined in a muffle furnace for six hours at 800 °C [2].

### **2.2.3. Sintering Process**

Sintering is a method that densifies porous materials by heating them to a specific temperature and transporting mass through the sample. Sintering requires a greater temperature than calcination. High temperature sintering causes grain thermal expansion, leading to reduced space between grains and a lower surface energy state in samples. Densified ceramics are the consequence of atoms on the grain surface being impacted by neighboring atoms in all directions during high temperature sintering. Sample density is influenced by several variables, including temperature, sintering time, volatile component evaporation, etc. Sample density is affected by temperature, sintering duration, and volatile constituent evaporation, among other parameters. Higher temperatures and longer sintering times lead to increased grain growth and larger grains. In the current work, the produced pellets of prepared material were sintered at 1173 K for 8 h [3].

## 2.3. Characterization Technique for the Synthesized Ceramic Materials

### 2.3.1. X-Ray Diffraction Analysis

X-ray diffraction (XRD) confirms the formation of crystalline phases in synthetic materials [3]. Each crystalline material has a distinct crystal imprint based on the atomic number and crystal planes involved. XRD gives a "fingerprint" of the crystalline substance.

X-ray diffraction assumes that a crystal is composed of a normal 3-dimensional array of atoms. The atoms in planes function as a 3-dimensional grating (Figure 2.6), scattering the incident X-ray beam in various directions.

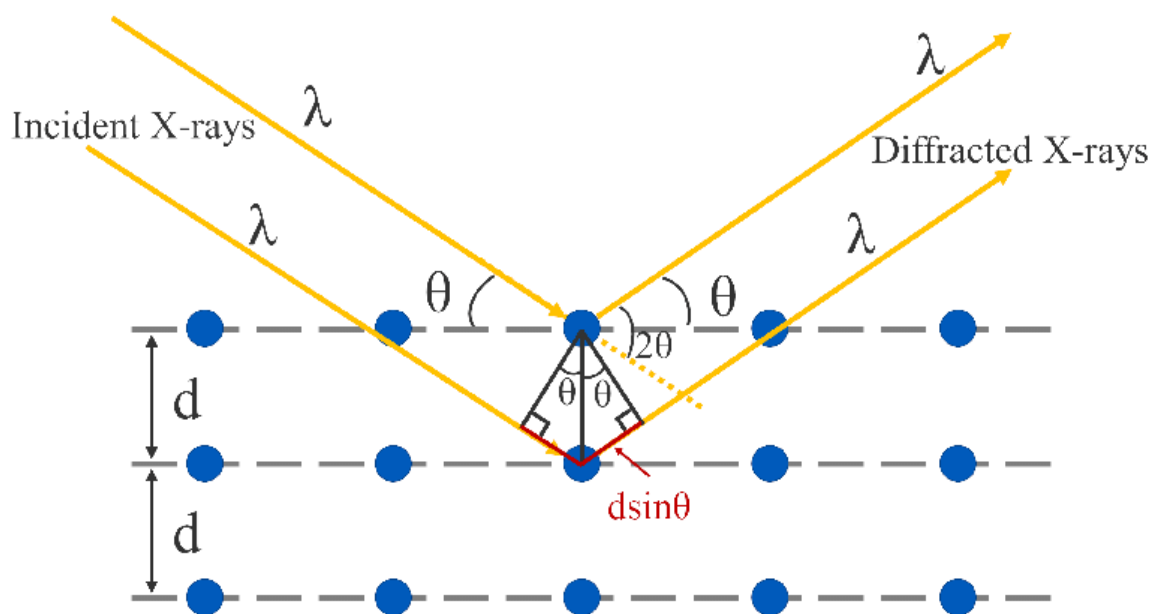


**Fig. 2.2.** Schematic representation of X-ray diffraction from crystal planes.

Scattering rays can cause both constructive and destructive interference. Constructive interference requires the following conditions:

The angle between incident and diffracted rays with normal to the surface must be the same.

The path difference between incident and diffracted rays must equal an integral multiple of the wavelength ( $\lambda$ ) of the X-ray utilized [4].

$$2d_{hkl}\sin\theta = n\lambda(n = 1,2,3 \dots) \quad 2.1$$

The equation above is known as Bragg's law, where  $\lambda$  represents the wavelength of the incident radiation,  $n$  represents the order of diffraction,  $d$  stands for the spacing between the crystal planes ( $hkl$ ), and  $\theta$  specifies the angle at which diffraction from these crystallographic planes is detected.

A crystal unit cell consists of three lattice parameters ( $a$ ,  $b$ , and  $c$ ) and three angle parameters ( $\alpha$ ,  $\beta$ , and  $\gamma$ ) between the axes. The unit cell characteristics of the material with cubic structure can be derived from the value of  $d$ -  $d$ -spacing using the formula:

$$\frac{1}{d_{hkl}^2} = \frac{h^2 + k^2 + l^2}{a^2} \quad 2.2$$

Since the XRD pattern provides structural information for bulk materials and thin films, as well as the composition of crystallographic phases in a sample. X-ray diffraction can be used to calculate the size of crystallites in materials using the Debye-Scherrer formula [5].

$$D = \frac{k\lambda}{\beta\cos\theta} \quad 2.3$$

where  $D$  represents particle size, and  $k$  stands for the Scherrer constant, typically around 0.9 for most crystals.  $\lambda$  denotes the X-ray wavelength,  $\beta$  signifies the full width at half maximum (FWHM), and  $\theta$  represents half of  $2\theta$  in the X-ray diffraction pattern of the material. In the experimental procedure, sintered pellets were initially crushed, and then powder X-ray diffraction patterns were obtained using a Rigaku miniflex 600 X-ray diffractometer from Japan. The scan rate was set at  $2^\circ/\text{min}$ , with a step size of 0.02, and Cu-K $\alpha$  radiation ( $\lambda=1.54059$  Å) was employed. Confirmation of the formation of a single-phase solid solution was achieved

by observing the absence of distinctive lines corresponding to constituent oxides or other compounds in the XRD patterns.



**Fig. 2.3.** Powder XRD instrument, Rigaku Miniflex 600 (Japan)

### 2.3.2. Scanning Electron Microscopy (SEM) Analysis

The scanning electron microscope (SEM) is an equipment that employs a high-energy electron beam instead of white light to examine the microstructure of materials. When electrons strike a substance, they emit secondary electrons, backscattered electrons (BSE), and characteristic X-rays. Secondary electron detectors are the most frequent type in all SEMs. Figure 3.3 depicts a schematic representation of the scanning electron microscope.

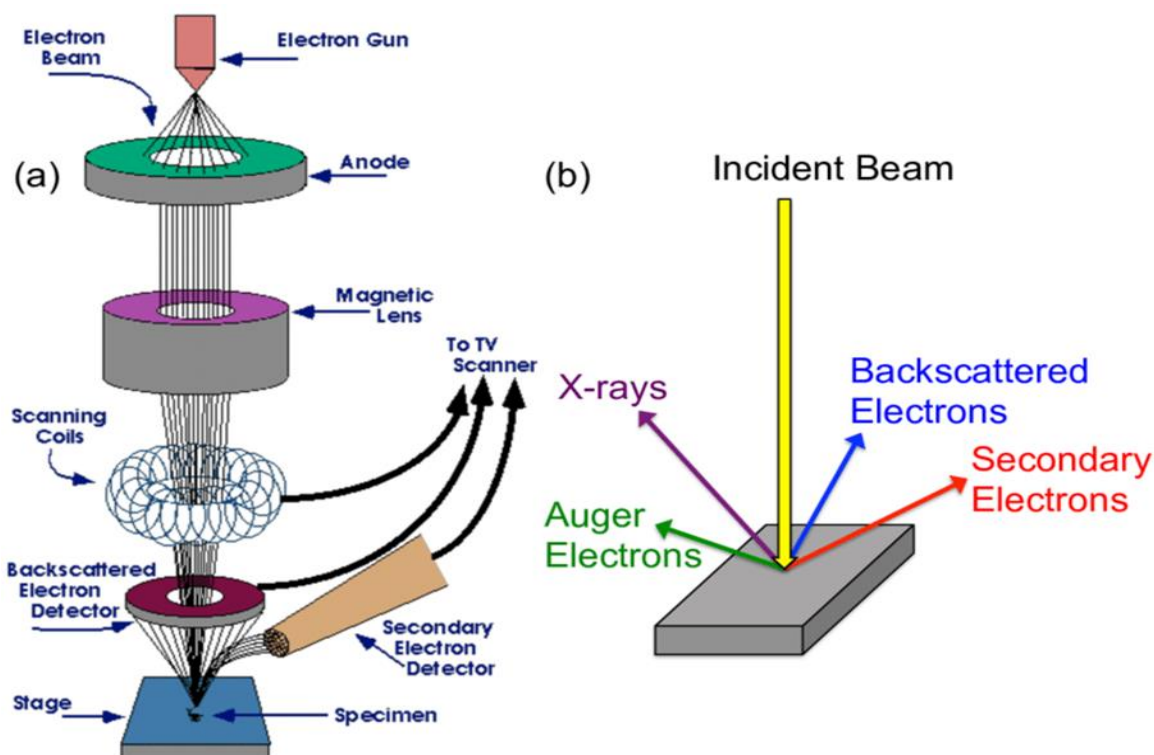


**Fig. 2.4.** Schematic representation of the Scanning Electron Microscope

The electron beam, pulsing with high energy, traverses vertically within the vacuum-sealed confines of the microscope. Along its path, it encounters electromagnetic fields and lenses meticulously crafted to focus its intensity onto the specimen. Guided by scanning coils, the beam bends along the x and y axes, methodically sweeping across the surface of the sample in a rectangular pattern. Upon contact with the sample, a cascade of electrons and X-rays is emitted. Sophisticated detectors capture these emissions—X-rays, backscattered electrons, and secondary electrons—and translate them into signals for transmission to the display apparatus. These signals originated from the interaction between electrons and the sample, yielding invaluable insights into its physical characteristics, unveiling details like surface texture, chemical composition, and the crystalline architecture and alignment of its constituent materials. SEM was used to investigate the dispersion homogeneity of the filler particles, the

size of the agglomeration, and the connectivity between filler particles. For SEM characterization, one of the non-conducting surfaces of the sintered pellets with appropriate thickness and diameter was polished using emery papers of different grades 0/0, 1/0, 2/0, 3/0, 4/0, and 5/0 successively to become smooth surface, afterward a thin layer of conducting materials such as gold or silver is deposited on the surface using a vacuum coating unit to obtain good image quality. Figure 3.4 depicts the use of a Scanning Electron Microscope (SEM) (Model JEOL JSM5410) at 20 kV in this study. SEM pictures of both cracked and etched surfaces were taken. For etching, the pellet's surface was treated with HF acid for a few seconds.



**Fig. 2.5.** Scanning Electron microscopy (SEM, ZEISS model, EVO18 Germany) and EDX Analysis instrument (Oxford instrument; USA)

### **2.3.3. Energy Dispersive X-ray Spectroscopy (EDX)**

Energy Dispersive X-ray spectroscopy (EDS or EDX) is a technique used in conjunction with scanning electron microscopy to evaluate the elemental and chemical compositions of the materials. It is based on how electromagnetic radiation interacts with matter. When the SEM

electron beam interacts with the sample, it causes the ejection of electrons from the atoms on the sample's surface. Subsequently, electrons from higher energy states occupy these vacancies, emitting an X-ray to equalize the energy disparity between the initial and final electron states. The emitted radiations (X-rays) from the samples are recorded and evaluated to determine the chemical composition and atoms present in the analyzed volume sample. EDX (Model JEOL JSM5410) analyzes the chemical composition and purity of materials.

#### **2.3.4. Transmission Electron Microscopy (TEM) Analysis**

Transmission electron microscopy (TEM) involves passing an electron beam through an ultra-thin object and interacting with it. Electrons transported through a specimen interact to create a picture, which is magnified and focussed on an imaging device such as a fluorescent screen. Since transmission electron microscopes have a smaller de Broglie wavelength than light microscopes, they can capture images at a much higher resolution. This allows the instrument to capture single atoms that are thousands of times smaller than an object that can be seen with a light microscope. It is a significant analytical technique in the fields of biological, physical, and chemical sciences. In addition to being helpful in many other domains including palynology and paleontology, it has numerous applications in the fields of virology, material science, cancer research, pollution, nanotechnology, and semiconductor research. The bright field TEM pictures and selected area diffraction patterns (SAED) were obtained using an FEI Tecnai-20G2 TEM with a 200 kV accelerating voltage and a LaB6 filament.

To perform TEM measurements, a small amount of fine ceramic powder was evenly dispersed in ethanol with a sonicator. A droplet of the resulting solution was deposited onto a carbon-coated copper grid and subsequently dried in the oven for 24 hours. The sample was then ready for TEM examination using the microscope. TEM micrographs show the nanocrystalline

character of the ceramic. The selection area electron diffraction pattern and HR-TEM results have been indexed using complex perovskite-based ceramics.



**Fig.2.6.** Transmission Electron Microscope (TEM, FEI TECANI G<sup>2</sup> 20 TWIN, USA) used to determine particle structure.

### **2.3.5. Atomic Force Microscopy (AFM) analysis**

Atomic force microscopy (AFM) is an advanced scanning probe microscopy (SPM) method capable of achieving resolutions on the scale of fractions of a nanometer, surpassing the optical diffraction limit by more than 1000 times. For this study, a Tapping mode Atomic Force Microscope (Bruker Dimension Edge with Scan Asyst) was employed to assess particle size distribution and average roughness. It has three major abilities such as force measurement, imaging, and manipulation.

### **2.3.6. Fourier Transform Infrared Spectroscopy (FT-IR)**

Fourier transform infrared (FT-IR) spectra were obtained using an ATR-FTIR spectrophotometer (Bruker, ALPHA model) in the range of 4000 cm<sup>-1</sup> to 500 cm<sup>-1</sup>. The

sample was mixed with solid KBr, crushed, and then compressed into a pellet using a hydraulic press. Each sample received an average of 64 scans at 4 cm<sup>-1</sup> resolution.

### **2.3.7. X-ray Photoelectron Spectroscopy (XPS)**

X-ray photoelectron spectroscopy (XPS), also known as electron spectroscopy for chemical analysis (ESCA), is a sensitive, non-destructive technique for determining the elemental composition and chemical state of samples by using thermos fisher scientific K $\alpha$  (Waltham, MA) in broad scan survey mode. Specimens were mounted on carbon tape or pellets (12 mm diameter) and analyzed overnight in a vacuum-sealed container. The measurement used monochromatic AlK $\alpha$  radiation (1486.6 eV) in ultra-high vacuum conditions. The binding energy of each element is scaled concerning the C 1s peak at 284.8 eV.

### **2.3.8. Electrical and dielectric measurements**

The LCR meter (PSM 1735, Newton 4th Ltd, U.K.) (Figure 3.5) was used to measure the dielectric properties as a function of frequency (100 Hz to 5 MHz) in the temperature range 300-500 K, using a bias voltage of 1 volt and a high-performance frequency LCR meter (E4980A/AL, Keysight, Malaysia) with a frequency range of 20 Hz to 2 MHz was also used. To determine the capacitance (C), resistance (R), and dielectric loss ( $\tan \delta$ ), dielectric electrical and impedance measurements were performed on sintered cylindrical pellet samples. To accomplish this, carefully polish the primary pellet faces to reduce the small curvature that is usual after sintering. These surfaces can act as electrodes when a tiny layer of conductive silver is applied to the pellet. Better electrical contact between the silver coating and the pellets can be attained by heating the pellets to a temperature exceeding 300 °C. The pellet holder used is a compression type, which allows the sample electrodes to be forced against the holder for secure electrical contact. To investigate the impact of temperature on dielectric characteristics,

pellets will be heated from room temperature to 600 K. This is accomplished by putting the pellet holder and pellets in a tube furnace that can be managed using a temperature controller. It was necessary to dwell the sample for 8-12 minutes before measuring it. To improve its thermal stability. To get more precise temperature settings, a thermocouple near the sample surface is used.

An alternating voltage signal (V) is applied between sample terminals at a specific test frequency. It measures the current (I) and phase angle ( $\theta$ ) between V and I. The collected values can be used to calculate the sample's complex impedance  $Z^*$  using the following equation:

$$Z^* = Z' - iZ'' \quad 2.4$$

with  $Z'' = Z \cos \theta$  is the imaginary part of impedance,  $Z' = Z \sin \theta$  is the real part of the complex impedance and  $Z = V/I$ .

The complex permittivity  $\epsilon^*$  is obtained as:

$$\epsilon^* = \epsilon' - i\epsilon'' = \frac{1}{i\omega C_0 Z^*} \quad 2.5$$

In this equation,  $\epsilon$ ,  $\epsilon'$ , and  $\omega$  have their usual meanings, and  $C_0 = \epsilon_0 A/d$ . The empty cell capacitance ( $d$ ) is calculated using A as the sample area and d as the sample thickness.

The real part of the complex permittivity (dielectric constant) is  $\epsilon' = Cd/\epsilon_0 A$ , where A is the area of the parallel plate capacitor and d is the plate separation. Dielectric loss is also known as  $\tan \delta$  which can be calculated by the ratio of the real and imaginary part of the dielectric constant and is defined as

$$\tan \delta = \frac{\epsilon''}{\epsilon'} \quad 2.6$$

The ac conductivity ( $\sigma_{ac}$ ) is another important property of material which reveals the conduction process involved in the material.  $\sigma_{ac}$  is calculated using the formula:

$$\sigma_{ac} = A\omega^n = \omega\varepsilon_0\varepsilon' \tan \delta \quad 2.7$$

where  $A'$  is a constant,  $\omega = 2\pi f$  is the angular frequency of the applied ac signal, and  $n$  is the frequency exponent. The variation of frequency exponent  $n$  with temperature indicates the type of conduction occurring.

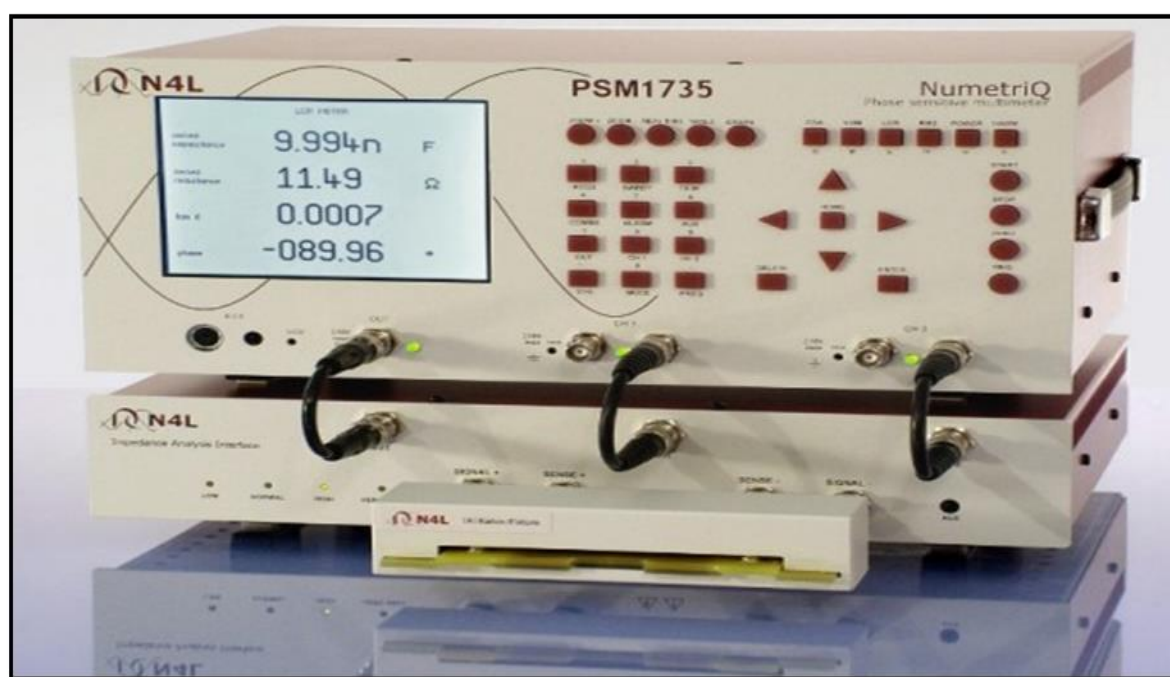


**Fig. 2.7** LCR Meter (PSM 1735, Newton 4th Ltd, U.K.) used for dielectric measurement

### 2.3.9. Impedance Spectroscopy (IS)

Impedance spectroscopy (IS) is a powerful tool used to examine relationships between electrical properties and the microstructural features of materials. Impedance spectroscopy measures the complex impedance ( $Z^*$ ) of the sample over a wide range of frequencies ( $10^2$  -  $10^6$  Hz) and temperatures (up to  $\sim 500$  K). However, for materials with high conductivity, sub-ambient tests are required to collect the necessary data. The electrical characteristics of a

material, influenced by extrinsic factors like electrode contact or grain boundaries which occur within the low-frequency range, approximately up to  $10^5$  Hz. Beyond this frequency, around  $10^5$  Hz and higher, the behavior may be attributed to the intrinsic factor within the bulk phase, such as lattice polarization or grain properties. Impedance spectroscopy analysis is based on the parallel combination of resistors and capacitors and the detailed discussion about impedance spectroscopy has been done in the introduction part.

## 2.4. References

- [1] V. Kumar, A Kumar, M. K. Verma, S. Singh, S Pandey, V. S. Rai, D. Prajapati, T. Das, N. B. Singh, K. D. Mandal, "Investigation of dielectric and electrochemical behavior of  $\text{CaCu}_{3-x}\text{Mn}_x\text{Ti}_4\text{O}_{12}$  ( $x=0, 1$ ) ceramic synthesized through semi-wet route," *Materials Chemistry and Physics*, **245** (2020) 122804.
- [2] Y. Xu, "Ferroelectric Materials and Their Applications," Elsevier Science, New York, (1991).
- [3] A. L. Maximenko, E. A. Olevsky, "Effective diffusion coefficients in solid-state sintering," *Acta materialia*, **52** (2004) 2953-2963.
- [4] A. A. Bunaciu, E. G. UdrişTioiu, H. Y. Aboul-Enein, Aboul-Enein, "X-ray diffraction: instrumentation and applications," *Critical reviews in analytical chemistry*, **45** (2015) 289-299.
- [5] U. Holzwarth, N. Gibson, "The Scherrer equation versus the 'Debye-Scherrer equation'." *Nature Nanotechnology*, **6** (2011) 534-534.
- [6] C. Kittel, "Introduction to Solid State Physics, Seventh Edition," John Wiley and Sons, Canada, (2006).
- [7] A. K. Jonscher, "The 'universal' dielectric response," *Nature*, **267** (1977) 673-679.